

Particle acceleration in supernova-remnant shocks

S.P. Reynolds

Abstract It has been known for over 50 years that the radio emission from shell supernova remnants (SNRs) indicates the presence of electrons with energies in the GeV range emitting synchrotron radiation. The discovery of nonthermal X-ray emission from supernova remnants is now 30 years old, and its interpretation as the extension of the radio synchrotron spectrum requires electrons with energies of up to 100 TeV. SNRs are now detected at GeV and TeV photon energies as well. Strong suggestions of the presence of energetic ions exist, but conclusive evidence remains elusive. Several arguments suggest that magnetic fields in SNRs are amplified by orders of magnitude from their values in the ambient interstellar medium. Supernova remnants are thus an excellent laboratory in which to study processes taking place in very high Mach-number shocks. I review the observations of high-energy emission from SNRs, and the theoretical framework in which those observations are interpreted.

1 Inferences from radio emission

Remnants of historical supernovae had been known since Lundmark's identification of the Crab Nebula with SN 1054 AD (Hubble 1928). The first radio source to be identified as a previously unknown supernova remnant (SNR) was Cassiopeia A, proposed by Shklovskii in 1953, who also suggested that synchrotron radiation was the mechanism for producing radio emission (Shklovskii 1953), based on the observed power-law spectrum $S_\nu \propto \nu^{-\alpha}$, with $\alpha \sim 0.8$ for Cas A. Minkowski in 1957 confirmed the identification from optical observations (Minkowski 1957). Thus from the early days of

radio astronomy, it was recognized that energetic particles were present in SNRs. Basic synchrotron physics tells us that emission at frequency ν is primarily by electrons with energy $E = 15(\nu(\text{GHz})/B(\mu\text{G}))^{1/2}$ GeV, so radio emission at frequencies of a few hundred MHz, typical at the time, immediately implied the presence of electrons with Lorentz factors of $10^3 - 10^4$.

Radio remains the spectral region in which SNRs are most consistently identified. Green's famous catalogue of Galactic SNRs (Green 2009; available online at <http://www.mrao.cam.ac.uk/surveys/snrs/>) lists 274 objects, essentially all with known radio properties. The mean spectral index is about 0.5, but with a significant spread of order 0.2 (Figure 1). This spread is a significant problem for theories of particle acceleration described below. Also significant is a tendency for the historical remnants (less than 2000 years old) to have steeper indices ($\alpha \gtrsim 0.6$), a trend continued by radio supernovae, not represented here, which can have indices as steep as 0.9 – 1.0 (Weiler et al. 2009). A few remnants such as Cas A have very well-sampled radio spectra (see references in Green 2009); Cas A's spectrum is well described by a single power-law with spectral index of 0.77 between 100 MHz and 100 GHz. However, most remnants are represented by only a few data points with substantial error bars. Other historical remnants have spectra with suggestions of concave-up curvature (Reynolds & Ellison 1992), naturally explained by efficient shock acceleration (see below).

Magnetic field strengths are difficult to measure in SNRs; since the intensity of synchrotron radiation from a power-law distribution of electrons $N(E) = KE^{-s}$ electrons $\text{cm}^{-3} \text{ erg}^{-1}$ scales as $KB^{1+\alpha}$, radio synchrotron fluxes only give roughly the product of the energy densities in magnetic field and electrons. X-ray evidence described below indicates that magnetic fields are substantially amplified over typical interstellar values of a few microGauss, but the only avenue

S.P. Reynolds

¹North Carolina State University

for estimating energetics from radio data is the use of minimum-energy equipartition arguments. These arguments indicate that the minimum energy in electrons and magnetic field in typical SNRs is far below the $\sim 10^{51}$ erg explosion energies; SNRs are not efficient synchrotron radiators. The equipartition magnetic fields so derived tend to be low, but as there is no strong physical argument that equipartition should hold, or even among which particles (should one include ions?), the equipartition magnetic field strength is really just a proxy for mean surface brightness.

Magnetic-field orientations can be usefully derived from radio polarization directions. A uniform synchrotron source with spectral index $\alpha = 0.5$ has a polarized fraction of about 70%, but very few remnants show values above 40%. Young SNRs have much lower values, typically of order 10% – 15% (see references in Reynolds & Gilmore 1993), implying that their magnetic fields are primarily disordered. The ordered components, however, tend to be radial. In older remnants, magnetic-field orientations are typically confused, but it is fairly common to see a tangential orientation, which one would expect if a high-compression radiative shock compresses upstream magnetic field, increasing the tangential component by a factor of the compression ratio.

Even though radio observations of SNRs do not require a large fraction of the SN energy, it is possible to argue that young SNRs require acceleration of new electrons – simply borrowing and compressing relativistic electrons from the cosmic-ray population in the ISM is inadequate both because of high observed surface brightnesses and spectra much different from those of low-energy cosmic-ray electrons (Reynolds 2008a).

Radio observations of SNRs have left several unexplained puzzles, most several decades old now. What is responsible for spectral indices flatter than 0.5? (While

a few pulsar-wind nebulae contaminate the low- α end of the distribution of Figure 1, most of the remnants with $\alpha < 0.5$ are shells.) In a few cases, contamination with flat-spectrum thermal emission may be responsible. Steeper spectra than 0.5 can be obtained with very low Mach-number shocks, but this requires $\mathcal{M} \lesssim 10$ and is unlikely to be the case for as many remnants as Figure 1 requires. Finally, the question of the radial orientation of the ordered component of magnetic field in young remnants remains unexplained, though the operation of fluid instabilities at the contact interface between shocked ISM and shocked ejecta is often invoked (e.g., Jun, Jones, & Norman 1996).

2 X-ray synchrotron emission

The featureless X-ray spectrum of the remnant of SN 1006 above 1 keV (Becker et al. 1980; Toor 1980) was first attributed to synchrotron radiation from shock-accelerated electrons by Reynolds & Chevalier (1981). This explanation required the presence of electrons with TeV energies. However, detection of oxygen lines from the spatially integrated spectrum (Galas et al. 1982) indicated the operation of thermal processes. Only with the ASCA observation of thermal line emission from the interior and a featureless continuum from the bright limbs (Koyama et al. 1995) was it clear that a synchrotron component was called for, though it represented the rolling off of the spectrum due to some process limiting the maximum energy of electrons, rather than to a straight extrapolation from radio (Reynolds 1996).

How do we know the featureless continuum emission is synchrotron radiation? Nothing else works. A nonthermal power-law electron distribution with energies of order tens of keV will produce a power-law bremsstrahlung spectrum with photon energies smaller by a factor of a few. However, those electrons would be just as efficient at exciting atomic lines as electrons drawn from a Maxwellian distribution. A tiny corner of parameter space might be available for a plasma either not yet ionized to the stages required for X-ray lines, or on the other hand totally stripped (e.g., Laming 1998). However, the careful study by Laming (1998) shows that in detail this cannot work for SN 1006. Finally, inverse-Compton upscattering of any known source of photons would produce a spectrum with the same slope as that of the synchrotron emission produced by those electrons – that is, the radio slope ($\alpha \sim 0.6$), far too flat for the observations ($\alpha_x \sim 2.3$; Long et al. 2003). Furthermore, the synchrotron hypothesis makes a prediction: spectral steepening to higher X-ray energies.

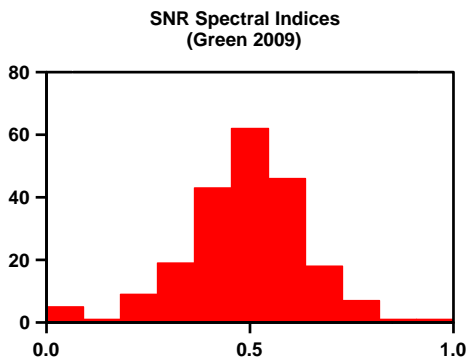


Fig. 1 Spectral-index distribution of SNRs in Green’s catalogue with adequately measured radio spectra, in bins of 0.1 in α .

For SN 1006, this has been confirmed by INTEGRAL (Kalemcı et al. 2006).

There are now four known Galactic remnants whose soft X-ray spectrum is dominated by synchrotron X-rays: in addition to SN 1006, G1.9+0.3 (Reynolds et al. 2008b); G347.3-0.5 (also known as GX J1713.7-3946 Slane et al. 1999); and G266.2-1.2, “Vela Jr.” (Aschenbach 1998; Slane et al. 2001). (See Reynolds 2008a for a more detailed review of SNR X-ray and γ -ray emission.) Figure 2 shows the *Chandra* images of SN 1006 and G1.9+0.3. For both objects, thermal lines have been detected from fainter regions of the remnant. The low-energy (central) emission in Fig. 2 is primarily ejecta emission dominated by oxygen. Figure 4 shows the spectrum from the interior of G1.9+0.3, with clear emission lines of Si, S, and Ar.

Synchrotron X-ray emission contributes to the spectrum of several more Galactic remnants (reviewed in Reynolds 2008a). In historical (or quasi-historical) remnants RCW 86 (SN 185?), Tycho (SN 1572), Kepler (SN 1604), and Cas A (SN \sim 1680), “thin rims” of featureless X-ray emission lie at the edges of the remnants, and are presumed to indicate the outer blast wave. Furthermore, all these remnants along with SN 1006 have been reported to have hard X-ray continua in integrated spectral (non-imaging) observations with the PCA instrument on RXTE (Allen, Gotthelf, & Petre 1999). It appears that synchrotron X-ray emission from the blast wave is a common feature in young SNRs, less than a few thousand years old. The implications are striking: electrons are present in these objects with energies $E = 72(h\nu/1 \text{ keV})^{1/2}(B/10 \mu\text{G})^{-1/2} \text{ TeV}$. Now the electron distributions are not straight power-laws all the way from radio-emitting energies (ca. 10 GeV); rather, in all known cases, the observed X-rays fall below that extrapolation (Reynolds & Keohane 1999), indicating that some limitation on electron energies is taking place below 100 TeV (perhaps far below, for those older SNRs with no evidence for synchrotron X-ray emission). As will be summarized below, shock acceleration may be limited by the finite age (or size) of the remnant, particle escape above some energy due to absence of scattering waves upstream, or (affecting electrons only) radiative losses.

3 Diffusive shock acceleration

In standard diffusive shock acceleration (amply reviewed in Blandford & Eichler 1987), particles scatter from magnetic inhomogeneities borne by converging fluids on either side of a shock wave, gaining energy with each reflection. Most particles disappear downstream

after each return, but a decreasing number remains for further cycles, producing a power-law distribution (see Bell 1978 for a kinetic-theory probabilistic argument). A well-known result of this process, for energetically unimportant test particles, is a power-law distribution with index dependent only on the shock compression ratio: $N(E) \propto E^{-s}$ with $s = (r + 2)/(r - 1)$ where $r \equiv \rho_2/\rho_1$ is the shock compression ratio, equal to 4 for strong shocks. This result applies to extreme-relativistic particles ($E \cong pc$, p the momentum and c the speed of light). The prediction is thus $s \cong 2$ which, for electrons, implies a synchrotron spectral index $\alpha = (s - 1)/2 = 0.5$, in tolerable agreement with spectra observed from Galactic SNRs.

The maximum energy to which particles can be accelerated depends on the limiting mechanism. We assume a diffusion coefficient κ which scales with particle energy. This results if the particle mean free path is a multiple η of its gyroradius: $\lambda_{\text{mfp}} = \eta r_g = \eta E/eB$ for ultrarelativistic particles, since $r_g = \gamma mc^2/eB$ (cgs units). Then the “Bohm limit” in which the mean free path is a gyroradius is $\eta = 1$. For weak turbulence, one expects $\eta \geq 1$, though this may not be a hard physical limit. For a remnant of age t with shock speed u_{sh} , with surroundings containing MHD scattering waves only up to a wavelength λ_{max} , the maximum energies scale as

$$E_{\text{max}}(\text{age}) \propto t u_{\text{sh}}^2 B \eta^{-1} \quad (1)$$

$$E_{\text{max}}(\text{escape}) \propto \lambda_{\text{max}} B \quad (2)$$

$$E_{\text{max}}(\text{loss}) \propto u_{\text{sh}} B^{-1/2} \eta^{-1/2} \quad (3)$$

In all cases, for $u_{\text{sh}} \gtrsim 1000 \text{ km s}^{-1}$ and ages above a few hundred years, maximum energies of 10 – 100 TeV are easily obtainable. The accelerated-particle spectra should show exponential cutoffs with these fiducial energies. For synchrotron emission, the dependence of the peak frequency ν_m on electron energy of $\nu_m \propto E^2$ means that the synchrotron spectrum will then drop roughly as $\nu^{-\sqrt{(E/E_{\text{max}})}}$, that is, considerably slower than exponential, and hardly differing from a power-law in the bandpass of most X-ray observatories ($\sim 0.3 - 10 \text{ keV}$).

The diffusion coefficient may be anisotropic; in particular, diffusion along and across magnetic-field lines is likely to take place at different rates, with effects on the acceleration time τ to some energy. If the shock velocity makes an angle θ_{Bn} with the mean upstream magnetic field, we can parameterize this effect with $R_J(\theta_{\text{Bn}}, \eta, r) \equiv \tau(\theta_{\text{Bn}})/\tau(\theta_{\text{Bn}} = 0)$. We scale to typical values for young SNRs: $u_{8.5} \equiv u_{\text{sh}}/3000 \text{ km s}^{-1}$; $t_3 \equiv t/1000 \text{ yr}$; $B_{10} \equiv B/10 \mu\text{G}$; and $\lambda_{17} \equiv \lambda_{\text{max}}/10^{17} \text{ cm}$. The frequencies at which electrons with energy E_{max} emit their peak power for each cutoff mechanism

are then

$$h\nu_{\text{roll}}(\text{age}) \sim 0.4 u_{8.5}^4 t_3^2 B_{10}^3 (\eta R_J)^{-2} \text{ keV} \quad (4)$$

$$h\nu_{\text{roll}}(\text{esc}) \sim 2 B_{10}^3 \lambda_{17}^2 \text{ keV} \quad (5)$$

$$h\nu_{\text{roll}}(\text{loss}) \sim 2 u_{8.5}^2 (\eta R_J)^{-1} \text{ keV}. \quad (6)$$

Of course, in a given object, the lowest value of E_{max} will be the operative value. Thus if one can determine the mechanism causing the spectral cutoff, its value constrains considerably more physical parameters than the simple observation of a radio power-law spectrum.

4 Radiation from GeV to TeV photon energies

Populations of relativistic ions and electrons can produce observable continuum radiation through four mechanisms, one hadronic and three leptonic (reviewed in Reynolds 2008a). The hadronic mechanism is the inelastic scattering of cosmic-ray protons on thermal nuclei, producing pions. The charged pions decay to electrons and positrons, making a (probably) negligible contribution to the relativistic lepton pool, but the π^0 's decay to gamma rays of comparable energy $E_\gamma(\text{min}) = m_\pi c^2/2 \sim 70 \text{ MeV}$. The spectrum of emitted photons should be that of the ions that produce them. The three leptonic processes are synchrotron emission, described above, as well as nonthermal bremsstrahlung, with the same spectrum as that of the nonthermal electrons, and inverse-Compton (IC) upscattering of photons from any significant ambient radiation. In practice, this is likely to be primarily the cosmic microwave background (CMB), though in some cases, IC from UV-optical-IR photons may be competitive. The spectrum will be the same as that of the synchrotron emission from whatever population of particles is responsible, that is, considerably harder in the keV – TeV range than that of the other processes. While the synchrotron process is clearly operating, it is not clear which of the other processes might be responsible for emission from any particular object. The best evidence for ion acceleration is the spectral feature resulting from the minimum photon energy from a created pion nearly at rest, about 70 MeV. Detailed calculations (e.g., Baring et al. 1999) show that this feature may not be highly distinct in a real object.

Several shell (i.e., not containing a pulsar) SNRs have been detected in TeV gamma rays, using air-Čerenkov detectors such as the High-Energy Stereoscopic System in Namibia. These include G347.3-0.5, Vela Jr., RCW 86, and SN 1006 (see references in Reynolds 2008a). The spectra are steep, with photon indices $\Gamma \sim 2$ ($F_\gamma \propto (h\nu)^{-\Gamma}$); for G347.3-0.5, the spectrum is observed to steepen above 1 TeV. Elaborate

models for these four cases have been constructed (e.g., Berezhko & Völk 2006). The TeV emission in these models can be due either to IC from the CMB, or to π^0 decay. Both classes of model have difficulty. The former require low filling factors of magnetic field, and imply inefficient shock acceleration, while the latter suffer from severe limits on thermal gas from X-ray observations, implying insufficient targets for the relativistic protons (Ellison et al. 2010). For complex objects such as G347.3-0.5 and Vela Jr., simple one-zone models may be inadequate, though there is as yet no clear path to consistent models.

5 Magnetic-field amplification

An important result first suggested many years ago, but only recently put on a firmer observational foundation, is the increase in magnetic-field strength in SNRs over a simple factor of the compression ratio expected in highly ionized gases. The possibility of much stronger shock amplification of magnetic fields was first proposed for heliospheric shocks by Chevalier (1977), while the models of Reynolds & Chevalier (1981) demanded substantial amplification. Early gamma-ray upper limits from Cas A bounded the electron population from above (from the inferred absence of bremsstrahlung), bounding the magnetic-field strength from below based on observed radio synchrotron fluxes. Cowsik & Sarkar (1980) used this argument to deduce a minimum magnetic field strength of about 1 mG. The slight concave curvature observed in radio spectra of SNRs was explained by Reynolds & Ellison (1992) as due to efficient shock acceleration modifying the shock structure, but values of magnetic field were also implied of 100 μG and more – far higher than a few times the typical interstellar magnetic field of 3 – 5 μG .

High-resolution X-ray images from *Chandra* show that the “thin rims” present in most historical shell SNRs are in fact very thin – so thin that an unusual depletion (beyond simple post-shock expansion) of either relativistic electrons or magnetic field is required to explain the sudden disappearance of synchrotron emissivity downstream (Bamba et al. 2003; Vink & Laming 2003). If synchrotron losses are depleting the electrons, we infer (Parizot et al. 2006)

$$B > 200 u_8^{2/3} (w/0.01 \text{ pc})^{-2/3} \mu\text{G} \quad (7)$$

where the shock speed $u_8 \equiv u/1000 \text{ km s}^{-1}$ and the filament width is w . However, if the amplified magnetic field is in waves of some kind, these waves might damp, providing an alternative mechanism for the rims (Pohl et al. 2005). Figure 3 shows a typical rim – but

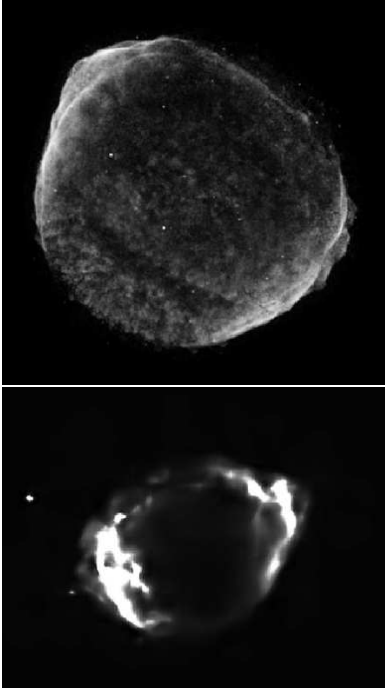


Fig. 2 *Chandra* images of (top) SN 1006 (NASA/CfA) and (bottom) G1.9+0.3 (Reynolds et al. 2008b) between 1.5 and 7 keV, smoothed with platelets as described in Willett (2007).

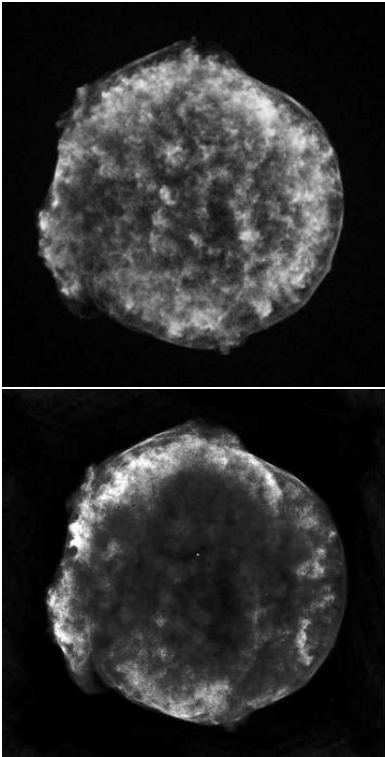


Fig. 3 Top: *Chandra* image of Tycho's SNR (NASA/CfA). Below: VLA image at 1.4 GHz (Reynoso et al. 1997). Note the thin rim in both bands at the NE edge (upper left).

it is present in radio as well, where synchrotron losses cannot possibly be a factor. It is possible that both mechanisms are required to explain some rims.

An additional argument for the amplification of magnetic field comes from the variations seen in periods of a few years in X-ray features in G347.3-0.5 (Uchiyama et al. 2007) and Cas A (Patnaude & Fesen 2007). Both brightening and fading are seen. If the relevant timescales are those of particle acceleration and synchrotron losses, in either case one obtains values of the magnetic field of order 1 mG. However, if the post-shock magnetic field is highly turbulent, one expects such “twinkling” due to fluctuations even if the mean magnetic field is lower (Bykov et al. 2008).

6 The youngest Galactic remnant G1.9+0.3

The discovery of a remnant only about 100 yr old, from expansion between radio observations made in 1985 and X-ray *Chandra* observations in 2007 (Reynolds et al. 2008b), opens a new window on the very early development of a SNR, and of the physics of unprecedentedly fast SNR shocks. At an assumed distance of the Galactic Center, 8.5 kpc (the very high absorbing column, $N_H \sim 6 \times 10^{22} \text{ cm}^{-2}$, means the distance cannot be much less), the mean expansion speed is about 14,000 km s^{-1} . The integrated synchrotron spectrum has a rolloff frequency of $h\nu = 2.2 \text{ keV}$, one of the highest ever measured. A recent longer observation has revealed the presence of spectral lines from the radio-bright N rim and interior (Figure 4).

The figure shows clear lines of helium-like states of Si, S, and Ar from the central region. Ca, while visible from the N rim, is absent in the center – but a line at 4.1 keV, which we identify as due to ^{44}Sc , is clearly present. ^{44}Sc is produced by electron capture in ^{44}Ti , a radioactive element with mean life of 89 yr. The inner-shell vacancy is filled by the emission of a 4.1 keV photon. This is the first firm detection of this element in a SNR.

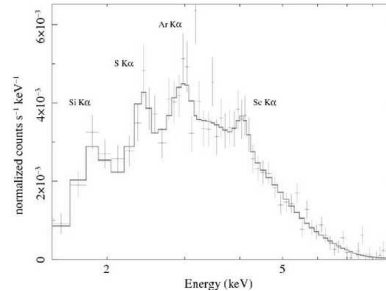


Fig. 4 Spectrum from the central region of G1.9+0.3 (Borkowski et al., in preparation).

The line strength we measure implies an initial mass of ^{44}Ti of $(1 - 3) \times 10^{-5} M_{\odot}$ for an age of 100 – 140 yr, within the predicted range for either core-collapse or Type Ia supernovae, though earlier spherically symmetric Type Ia models predict lower ^{44}Ti masses. Since the ^{44}Sc need not be ionized to produce the 4.1 keV X-rays, we are sensitive to both shocked and unshocked ^{44}Sc . A longer observation can allow the determination of the spatial distribution and kinematics of ^{44}Ti , of considerable interest to SN modelers.

7 Status report

1. X-ray observations show that SNR shocks routinely exhibit synchrotron radiation from electrons up to 100 TeV in energy.
2. Standard diffusive shock acceleration can easily account for these energies for a range of conditions. Little, however, can be predicted. Quantities of interest include efficiencies, obliquity-dependence (i.e., θ_{Bn} -dependence), or e/p ratio.
3. Emission at TeV energies seen from several young SNRs may be leptonic (IC/CMB) or hadronic (π^0 -decay). Both types of models have serious problems. In particular, while many indirect lines of evidence suggest that these shocks efficiently accelerate ions, direct observational confirmation is still lacking.
4. Both integrated fluxes and small-scale structure in X-rays indicate that magnetic fields in SNRs are higher by 10 – 100 than expected from simple compression of ISM fields. This may be due to a cosmic-ray driven instability (Bell 2004). This instability requires high-efficiency ion acceleration.
5. Future needs: Observations at GeV energies (and, we hope, down to 100 MeV or below) with the *Fermi* Gamma-Ray Space Telescope will be important in constraining models. Theoretical work to predict how particles are injected into the shock-acceleration process as well as the items enumerated above is essential. Radio observations provide information which has still not been used by modelers to maximum effect. Finally, G1.9+0.3 is evolving so quickly that its monitoring with time, and the accumulation of better statistics for spectroscopy, may add substantially to our understanding of shock acceleration in young SNRs.

Acknowledgements

I gratefully acknowledge support from NASA and NSF for supernova-remnant research.

References

- Allen, G.E., Gotthelf, E.V., & Petre, R. 1999, *Proc. 26th ICRC*, 3, 480
- Aschenbach, B. 1998, *Nature*, 396, 141
- Bamba, A., et al. 2003, *ApJ*, 589, 827
- Baring, M.G., et al. 1999, *ApJ*, 513, 311
- Becker, R.H., et al. 1980, *ApJ*, 240, L33
- Bell, A.R. 1978, *MNRAS*, 182, 147
- Bell, A.R. 2004, *MNRAS*, 353, 550
- Berezhko, E.G., & Völk, H. 2006, *A&A*, 451, 981
- Blandford, R.D., & Eichler, D. 1987, *Phys.Rep.*, 154, 1
- Bykov, A.M., et al. 2008, *ApJ*, 689, L133
- Chevalier, R.A. 1977, *Nature*, 266, 701
- Cowsik, R., & Sarkar, S. 1980, *MNRAS*, 191, 855
- Ellison, D.C., et al. 2010, *ApJ*, 712, 287
- Galas, C.M.F., Venkatesan, D., & Garmire, G. 1982, *Ap.Lett.*, 22, 103
- Green, D.A. 2009, “A Catalogue of Galactic Supernova Remnants (2009 March version)”, Astrophysics Group, Cavendish Laboratory, Cambridge, UK
- Hubble, E. 1928, *Astr.Soc.Pacific Leaflet #14*
- Jun, B.-I., Jones, T.W., & Norman, M.L. 1996, *ApJ*, 468, L59
- Kalemci, E., et al. 2006, *ApJ*, 644, 274
- Koyama, K., et al. 1995, *Nature*, 378, 255
- Laming, J.M. 1998, *ApJ*, 499, 309
- Long, K.S., et al. 2003, *ApJ*, 586, 1162
- Minkowski, R. 1957, *Proc.IAU Symp.#4*, ed. H.C.van de Hulst (Cambridge: Cambridge U. Press), 107
- Parizot, E., et al. 2006, *A&A*, 453, 387
- Patnaude, D.J., & Fesen, R.A. 2007, *AJ*, 133, 147
- Pohl, M., et al. 2005, *ApJ*, 626, L101
- Reynolds, S.P. 1996, *ApJ*, 459, L13
- Reynolds, S.P. 2008a, *ARA&A*, 46, 89
- Reynolds, S.P. et al. 2008b, *ApJ*, 680, L41
- Reynolds, S.P., & Chevalier, R.A. 1981, *ApJ*, 245, 912
- Reynolds, S.P., & Ellison, D.C. 1992, *ApJ*, 399, L75
- Reynolds, S.P., & Gilmore, D.M. 1993, *AJ*, 106, 272
- Reynolds, S.P., & Keohane, J.M. 1999, 525, 368
- Reynoso, E., et al. 1997, *ApJ*, 491, 816
- Shklovskii, I.S. 1953, *Dokl.Akad.Nauk.SSSR* 91, 475
- Slane, P.O., et al. 1999, *ApJ*, 525, 357
- Slane, P.O., et al. 2001, *ApJ*, 548, 814
- Toor, A. 1980, *A&A*, 85, 184
- Uchiyama, Y., et al. 2007, *Nature*, 449, 576
- Vink, J., & Laming, J.M. 2003, *ApJ*, 584, 758
- Weiler, K.W., et al. 2009, *AIP Conf.Proc.*, 1111, 440
- Willett, R. 2007, in *Statistical Challenges in Modern Astronomy IV*, eds. G.J. Babu & E.D. Feigelson, *APS Conf. Ser.* 371, 247